A mass budget and box model of global plastics cycling, degradation and dispersal in the land-ocean-atmosphere system

Jeroen E. Sonke[1]*, Alkuin Koenig[2], Nadiia Yakovenko[1], Oskar Hagelskjær[1,3], Henar Margenat[3], Sophia V. Hansson[3], Francois De Vleeschouwer[4], Olivier Magand[2], Gael Le Roux[3], Jennie L. Thomas[2]

[1] Géosciences Environnement Toulouse, CNRS/IRD/Université Paul Sabatier Toulouse 3, Toulouse, France

[2] Institut des Géosciences de l'Environnement, Univ. Grenoble Alpes, CNRS, IRD, Grenoble INP, Grenoble, France

[3] Laboratoire écologie fonctionnelle et environnement, CNRS/INP/Université de Toulouse, Av. de l'Agrobiopole, 31326 Toulouse, France

[4] Instituto Franco-Argentino para el Estudio del Clima y sus Impactos (UMI 3351 IFAECI/CNRS-CONICET-UBA-IRD), Universidad de Buenos Aires, Buenos Aires, Argentina

*Corresponding author: jeroen.sonke@get.omp.eu

Keywords: microplastics, fluxes, emission, deposition, river, ocean, beach, sediment, soil, waste

List of Abbreviations

Tg, teragrams
P, macroplastics
LMP, large microplastics
SMP, small microplastics
y, year
F, flux (in Tg y^{-1})
M, mass (in Tg)
1σ, one (sigma) standard deviation
BAU, business as usual
SCS, systems change scenario

Abstract

Since 1950 humans have introduced 8300 teragrams (Tg, 10^{12} grams, millions of metric tons) of plastic polymers into the Earth's surface environment. Accounting for the dispersal and fate of produced plastics and fragmented microplastics in the environment has been challenging. Recent studies have fueled debate on the global river budget for plastic transport to oceans, the sinking and beaching of marine plastics and the emission and deposition of atmospheric microplastics. Here we define a global plastics cycle and budget, and develop a box model of plastic cycling, including the fragmentation and transport of large and small microplastics (LMP, SMP) within coupled terrestrial, oceanic and atmospheric reservoirs. We force the model with historical plastics production and waste data, and explore how macroplastics, LMP and SMP propagate through the reservoirs from 1950 to 2015 and beyond. We find that considerable amounts of plastics reside most likely in the deep ocean (82 Tg), in shelf sediments (116 Tg), on beaches (1.8 Tg) and, as a result of marine emissions, in the remote terrestrial surface pool (28 Tg). Business as usual or maximum feasible reduction and discard scenarios show similar, 4-fold increases in atmospheric and aquatic ecosystem SMP exposure by 2050, because future plastics mobilization is controlled by releases from the large terrestrial discarded plastics reservoir (3500 Tg). Zero-release from 2025 onwards illustrates recovery of P and LMP reservoirs on centennial time scales, while SMP continue to cycle in air, soil, and surface ocean for millennia. Limiting dramatic future dispersal of plastics requires, in addition to reducing use and waste, remediation of the large terrestrial legacy plastics pool.

Introduction

A characteristic feature of the Anthropocene is the widespread dispersal of plastic polymers across Earth's surface since the 1950s (1). Of the 1.5 trillion barrels of oil (200,000 Tg) produced since the 1950s (2) about 4% (8300 Tg) has been transformed into non-biodegradable polymers, and used in predominantly single-use packaging or short-lived (1-25y) technological applications (3). Produced plastics have been abundantly

(60%) discarded into the technosphere, the part of the environment that has been made or modified by humans: urban, sub-urban, agricultural, and industrial areas, including landfills (3,4). The pool of discarded managed and mismanaged plastic waste has been slowly mobilized by wind, runoff, rivers and ocean currents to all remote corners of planet Earth, including the poles and the deep ocean (5–8). Large plastic debris tend to fragment to micro- and nano-sized particles, which due to their increased surface area can absorb, adsorb or release a range of secondary natural and man-made chemical compounds in the environment (9). Assessing the possible impact of plastics on ecosystem and human health, and mitigating this impact, requires a solid understanding of where and when discarded plastics end-up, and to which size range they evolve.

Over the past decades important efforts have been made to chart the abundance, size properties, and bulk polymer composition of plastics in the surface ocean, soils, rivers, wetlands, biota and atmosphere. A perceived mismatch between the relatively small quantity of plastics in the surface ocean (0.3 Tg) (10) and the large quantity delivered by global rivers (4.8 – 12.7 Tg y^{-1}) (11) has fueled a 'missing marine plastics' paradox (12). Solutions to this issue have been proposed in the transfer of marine plastics to the deep ocean (13,14), to coastal environments, via beaching (15,16), to the subsurface ocean and marine sediments by sinking (17,18), and to marine emission of microplastics to the atmosphere (19,20). Recently, a 1000-fold lower global river flux of 0.0064 Tg y^{-1} was suggested, based on an alternative median plastics mass (21). Such a low river flux would imply a marine residence time of several years, and possibly removes the need for a missing marine plastics sink. In parallel to rivers and ocean currents, the atmosphere has been identified as a global vector of MP, in both urban (22,23) and remote environments (5,24,25), including MP emission from land (19,26) and sea (19,20). In this study we use the best available estimates of both plastics abundance and fluxes to construct a global plastics mass budget. This budget is implemented in a global box model of plastics cycling between land, atmosphere and ocean from 1950 to 2015. We then use the model to explore how plastics disperse through Earth's surface environment over times scale ranging from decades, focusing on policy scenarios, to millennia, addressing the fate and potential burden of global plastics contamination.

Plastics cycling box model

In order to construct a global plastics mass and mass transfer budget (Figure 1), we use plastics observations from the literature and a box modeling approach (see Methods for details). We subdivide macroplastics (P, >5mm), large microplastics (LMP, >0.3mm and <5mm) and small microplastics (SMP, <0.3mm), and define 'MP' as the sum of LMP plus SMP. The GBM-Plastics model (version 1.0) is a coupled 15-reservoir numerical box model that simulates how produced P and MP propagate through the terrestrial, marine, and atmospheric environments upon release or emission. P fragment to LMP, and LMP fragment to SMP, and only SMP become airborne, emitted from and deposited to oceans and land. Terminal P, LMP and SMP sinks are marine sediments, whereas remote terrestrial (soils, barren rock, ice sheets) and deep ocean pools act as long-term temporary reservoirs. The mass flux, F_{ab} (Tg y^{-1}) between two reservoirs a and b is $F_{ab} = k_{ab} \times M_a$, where M_a is the mass of plastics in reservoir *a* (Tg), and k_{ab} is a first-order mass transfer (rate) coefficient (y^{-1}). In such a first-order mass transfer model, an increase in mass of reservoir 'a' leads to a proportional (by 'k_{ab}') increase of the flux, F_{ab}, to reservoir b, and a consequent proportional increase in the mass of reservoir 'b'. In order to derive the k's one must know, for a given year or reasonably short period of observation, the magnitudes of F and M. Alternatively, some k's can be derived experimentally, such as plastics sedimentation rates, with units y^{-1}, or from theory. Therefore, in a first step, we calculate most k values from published, recent, 2005-2022 observations (see Methods) and from model estimates of atmospheric SMP fluxes (19). The model is then run from 1950 to 2015, with only the k_{ab} transfer coefficients and plastics production and waste generation as external forcing. In the following we discuss whether the simulated modern plastics distribution for 2015 corresponds to observations, which k values (and therefore fluxes) need to be adjusted, and what the model implications are for our understanding of plastic cycling. With the addition of atmospheric transport of plastics, the term 'emission' refers here exclusively to the suspension of terrestrial and marine SMP in air. 'Release' is used as the generic term for plastics discharge and mobilization to the technosphere and in-land aquatic and marine environments. Conversion of plastics number concentration to mass concentration is detailed in the Methods. All uncertainties reported are 1σ standard deviation (or 16^{th} and 84^{th} percentiles, corresponding to a 1σ uncertainty; see Methods).

We start by detailing the 'base case' plastics cycling model, based on best known modern observations of reservoir sizes and fluxes between reservoirs (see Methods for details). We include plastics production (8300 Tg since 1950), waste generation and waste disposal from Geyer et al. (3) who estimated 2600 Tg of

plastics to be in use in 2015, 4900 Tg discarded (split into 4200 Tg of P, and 700 of primary LMP following Lau et al. (4) and 800 Tg incinerated. In the base case we use the mid-point of the river plastics flux estimate by Jambeck et al., of 8.5 Tg y^{-1} (11), containing equal fractions of P and LMP. We adopt surface ocean mixed layer buoyant P and LMP inventories of 0.23 and 0.04 Tg (10), and a surface mixed layer SMP inventory of 0.003 Tg (27). We make an order of magnitude estimate of beached LMP of 0.5 ± 0.4 Tg, based on the global surface of sandy beaches (2.63 10^5 km^2; (28)), a median global beach sand LMP abundance of 2450 MP km^{-2}, and median beached LMP size of 2.0 mm (29). We estimate beached P, and shelf sediment P pools from a review study (30) that estimates mean beached P and sea floor P concentrations of 2 and 5 Mg km^{-2} respectively (uncertainty not estimated). Multiplying by beach and continental shelf surfaces of 2.63 10^5 and 2.89 10^7 km^2 results in beached and shelf sediment P pools of 1.3 and 51 Tg. An estimate for the global deep ocean sediment MP pool of 1.5 Tg is based on observed mean deep sediment MP concentrations of 0.72 MP g^{-1} (see Methods) (31). A shelf sediment MP pool of 65 Tg (1σ, 21 to 78Tg) is estimated from subtidal sediment median MP concentrations of 100 MP kg^{-1} (see Methods) (29). Rate coefficients for P and LMP beaching (the transfer from ocean to beach), $k_{beaching}$ of 0.15 y^{-1} are approximated based on Onink et al. (15). Surface mixed layer to deep subsurface ocean sinking rates of P, LMP, SMP lack *in situ* observations; we estimate model sinking rate coefficients, $k_{P,sinking}$ of 1367 y^{-1}, $k_{LMP,sinking}$ of 196 y^{-1} and $k_{SMP,sinking}$ of 33 y^{-1} for the 100 m deep surface ocean mixed layer, based on the empirical results of a sinking tank study of mixed phytoplankton aggregates with MP(17). We include the sinking and sedimentation of non-buoyant P over the shelf, but not from open ocean waters, assuming that only buoyant P dominate open ocean P. Macroplastics, P, are beached as described above, and fragmented in surface ocean waters to LMP at a rate $k_{oceP \rightarrow LMP}$ of 0.03 y^{-1} (16), supported by observations (32). A recent review of plastics degradation rates highlights the complexity and variability of plastics degradation rates as a function of polymer type, sunlight, and physical environment (33). The authors use an observed median HDPE degradation rate of 4.3 μm y^{-1} in the marine environment, and a theoretical degradation framework to illustrate how a typical HDEP bag (film), fiber (2 mm diameter, 230mm long) or bead (8.8 mm diameter) would degrade at relative mass loss rates of 0.5, 0.005 and 0.0014 y^{-1}. The rate of 0.03 y^{-1} (1σ uncertainty: 0.006 to 0.06 y^{-1}) we adopt lies within this estimated variability. We consider that for the purpose of our study, it is too early at present to try and incorporate more detailed plastics fragmentation or degradation parameterizations. We agree with Chamas et al. (33) that more robust degradation observations are needed, and we suggest that a follow-up box model that incorporates variable polymer types would be a more appropriate occasion. In the absence of fragmentation rates for LMP to SMP in surface, subsurface waters, beach zone, and discarded pool, and for P to LMP in subsurface water, beach zone and discarded pool we adopt, in the base case, the same rate $k_{oceLMP \rightarrow SMP}$ of 0.03 y^{-1} for all these fragmentation sites.

The subsurface ocean pool of LMP and SMP, below the surface mixed layer, is of importance to complete the marine plastics budget and to parameterize model settling and sedimentation of plastics. Table 1 and Figure 2 summarize recent observations of subsurface marine MP. We estimate a global deep ocean MP inventory of 82 ± 47 Tg based on mean N-Pacific pelagic concentrations of 131 ± 44 μg m^{-3} (6,34), mean N and S-Atlantic concentrations of 91 ± 46 μg m^{-3} (35–37), and extrapolated estimates for the Indian, Southern, and S-Pacific Oceans (Table 2, Methods).

Recent studies on atmospheric MP cycling show fragment and fiber size distributions to be in the SMP range <300 μm. While LMP emission and deposition occurs, these tend to deposit more rapidly back to the same reservoir (e.g., marine emission followed by marine deposition) and are therefore ignored in the box model. Table 3 summarizes SMP observations in the boundary layer and free troposphere, yielding a total tropospheric SMP mass of 0.031 ± 0.027 Tg. This observed stock is 10x higher, though within uncertainty, of a model estimate of 0.0036 Tg (19). Our estimate of 0.031 Tg is very sensitive to the assumed median SMP size of 70 μm, which is where the atmospheric SMP model allocates most SMP mass (19). We adopt global SMP emissions from the same model study (19): emissions from roads, 0.1 Tg y^{-1}, agricultural dust, 0.07 Tg y^{-1}, population dust, 0.02 Tg y^{-1}, and oceans, 8.6 Tg y^{-1}. We use SMP deposition observations over land (5,24,38) in combination with population density data for 2015 (39) to estimate global SMP deposition over land of 1.1 ± 0.3 Tg y^{-1} and an accumulated remote terrestrial SMP pool of 28 ± 10 Tg (see Methods). We assume that global SMP emissions (8.6 Tg y^{-1}; (19)) equal deposition, and estimate SMP deposition over oceans as the difference between total deposition and deposition over land: 7.6 Tg y^{-1}. This large re-deposition of SMP over the ocean is coherent with the short, 2.4 h, lifetime of the coarsest, 70 μm SMP size fraction that represents 85% or marine SMP emission in the model of ref (40).

Results and Discussion

The box model 'base case' is run from 1950 to 2015 and results, in terms of plastics reservoir sizes and fluxes for the year 2015, are shown in Table 4 in comparison to the above-mentioned observations. The base case reproduces observed amounts of in-use P, discarded P, LMP, SMP and terrestrial SMP to within 40%. Using the mid-point river plastics flux of 8.5 Tg y^{-1} (11) the base case also reproduces well the observed downstream plastics mass in marine and remote terrestrial systems (surface and deep ocean, sediments, beach, remote terrestrial surfaces) of 201 Tg (1σ, 120 to 630 Tg). Remote terrestrial surfaces are included in the downstream environment, because its accumulated SMP mass is for 96% derived from the SMP river flux, surface ocean LMP degradation, and the important marine emission of SMP to the atmosphere where it leads to global dispersal and deposition to remote terrestrial surfaces (soil, rock, deserts, ice). We note that using the 2000-fold lower river plastics flux of 0.0064 Tg y^{-1} by Weiss et al. (21) would lead to important low bias in the marine and remote terrestrial reservoirs. A model river plastics flux of 13 Tg y^{-1} (1σ, 9 to 51 Tg) balances the overall marine plastics budget, and gives satisfactory (within a factor 10x) reproduction of surface ocean P, LMP and SMP, shelf sediment P, LMP and SMP, and beached LMP reservoirs. Within the marine system, the modeled deep sediment MP pool is however biased high 90-fold, and beached P biased low 26-fold, exceeding the 10x uncertainty we apply to the observed pools. We therefore optimize and lower subsurface ocean specific $k_{LMP,sinking}$ from 4.9 y^{-1} to 0.0012 y^{-1} and $k_{SMP,sinking}$ from 0.8 y^{-1} to 0.0002 y^{-1}, and increase $k_{beaching}$ from 0.15 y^{-1} to 4.0 y^{-1}. We argue that the base case sinking rates and k estimates for experimental biofouled LMP and SMP are inappropriate for deep ocean sedimentation because remineralization of biofilm during sinking increases buoyancy, halts sinking and lowers the effective sinking rate (14). The base case $k_{beaching}$ was derived for the coastal ocean (15), which we do not explicitly separate and simulate here, likely leading to its underestimation relative to whole surface ocean P cycling. It is important to note that out of 23 mass transfer coefficients (k's) only 2 needed fitting in the 'base case'. This indicates that current understanding of P, LMP and SMP stocks and fluxes, which determine k's, is sufficiently accurate to formulate and use the box model.

Figure 1 presents our best estimate of the global plastics cycle for the year 2015, based on observed inventories and fluxes (black), modeled inventories and fluxes (red), including the modeled river plastics flux of 13 Tg y^{-1} to the ocean (see Table 4 for uncertainties). Key properties of the global plastics cycle are:

1. The large mass, 1200 Tg of discarded LMP (of which 840 Tg primary LMP) and on the order of 540 Tg of discarded SMP in the technosphere, which are potentially mobilizable to wetlands, oceans, groundwater, atmosphere and remote terrestrial surfaces.
2. The substantial mass of plastics, 201 Tg, representing 3% of all plastics produced since 1950, that has been released from the technosphere to pristine terrestrial and marine ecosystems.
3. The 65-fold larger river plastics flux (13 Tg y^{-1}) compared to the total terrestrial atmospheric SMP emission flux (0.2 Tg y^{-1}).
4. The importance of marine SMP emissions on further distributing microplastics to remote ocean waters and to remote terrestrial surfaces (96% of the 28 Tg on remote land originates from marine emissions, and only 4% from terrestrial emissions).
5. The potentially large subsurface oceanic LMP and SMP (82 ± 47 Tg), and shelf sediment P and LMP (116 Tg) reservoirs, compared to beached P and LMP (1.8 Tg), and compared to surface ocean plastics (0.27 Tg).

The uncertainties associated with the global plastics cycle (Table 4) are large, due to an overall lack of observations and underlying plastics quantification challenges. In particular, observations of SMP number and mass in the terrestrial discarded and remote terrestrial pools, and in terrestrial and marine emissions and deposition are needed.

We use the box model to simulate and illustrate at what timescales P, LMP and SMP propagate through Earth surface reservoirs if we were to halt plastics production and waste generation in 2025. While such a scenario is not realistic, it serves to understand the timescales involved in plastics dispersal and degradation across the Earth's surface. Figure 3 shows P, LMP and SMP dispersal from 1950 to the year 3000 (see also SI 2 for model data output): The discarded terrestrial P pool decreases rapidly, by 90% in 2100, due to fragmentation to LMP, which in turn decreases by 90% in 2150 due to further fragmentation to SMP. LMP and SMP transport by rivers and air leads to rapid increases of LMP and SMP in the marine pools and of SMP in the remote terrestrial pool. The discarded SMP pool takes longer, 90% by 2500, to mobilize to the surface ocean, and from there via marine emission back to the remote terrestrial pool. The cyclical behavior that

develops, cycles SMP for millennia back and forth between surface ocean and continents, before gradual escape of SMP to the deep ocean marine sediments (Figure 4). This scenario illustrates that even if we would entirely replace plastics by alternative materials, the legacy of historical plastics mismanagement could result in prolonged plastics dispersal over centuries (LMP) or millennia (SMP), unless we better manage present and future discarded plastics pools on land. I should be noted that the relevance of persistent SMP cycling over millennial timescales will depend on their degradation to nanoplastics, and eventually to dissolved monomers that serve as carbon substrates to biological organisms.

Next, we explore in detail how two more realistic production and waste management scenarios affect plastics cycling over the period 2015 to 2050 (Figure 5 and SI 2): 1. The business as usual (BAU) scenario from Geyer et al. (3) reaching 30,000 Tg of produced plastics in 2050, and with discard below 10% and recycling and incineration of 43% and 49% in 2050, 2. The systems change scenario (SCS) from Lau et al. (4) which proposes ambitious, but realistic measures to reduce, substitute, recycle, and dispose of plastics (see Methods for details, and SI 2). Figure 5A illustrates how a 2-fold drop in plastics production from 550 Tg y^{-1} to 250 Tg y^{-1} in 2040 under the SCS scenario significantly limits further plastics accumulation in the technosphere compared to BAU. Yet, despite the projected strong decrease of mismanaged waste, and increase in safe disposal and recycling, the SCS does not lead to measurable changes in key metrics, such as beached P, total river plastics flux (P+LMP+SMP) or atmospheric SMP deposition to remote terrestrial surfaces by 2050 (Figure 5 B, C, D). The reason for this is the persistent mobility of legacy plastic waste in the large terrestrial discarded P, LMP and SMP reservoirs. To render SCS policy effective, it will have to be supported by immobilization or remediation of the terrestrial discarded plastics pool. We explore the potential impact of remediation of the discarded P pool from 2025 onwards at a rate of 3% P isolation and safe disposal per year (Figure 5 B, C, D). Discarded P remediation halts beached P dispersal by 2040, curbs total river plastics discharge to some extent but does not impact atmospheric SMP deposition to land. Although technically more challenging, remediation of discarded LMP and SMP pools on land at an identical 3% per year rate is needed to also inverse dispersal of river and atmospheric plastics (Figure 5 B, C, D) and to truly limit future planetary dispersal of plastics. The current clean-up initiative of surface ocean plastics does not sufficiently address the long-term mobilization of the legacy plastics pool on land. The fragmentation of SMP to nanoplastics and ultimately to dissolved and colloidal polymers, that are energy sources to microbes needs further study, in particular their rates of production, before they can be included in the box model. Engineered LMP and SMP biodegradation could be a solution to the suggested need for remediation of these legacy pools on land.

Conclusions

In this study we define a global plastics cycling budget for the year 2015, and develop a box model of plastic cycling, including the transport and fragmentation of macroplastics (P) to large (LMP) and to small microplastics (SMP) within coupled terrestrial, oceanic and atmospheric reservoirs. We drive the model with historical plastics production and waste data, and investigate how macroplastics (P), LMP and SMP propagate through Earth surface reservoirs from 1950 to 2015 and beyond, to 2050 and to the year 3000. Based on published plastics observations we estimate that important amounts of plastics are present in the deep ocean (82 Tg), in shelf sediments (116 Tg), on beaches (1.8 Tg) and in the remote terrestrial surface pool (28 Tg). The box model suggests that plastics in the remote terrestrial surface pool originate predominantly from marine SMP emissions that are transported via the atmosphere and deposited over land. Simulated zero-release of plastics to land, water and air from 2025 onwards illustrates how P and LMP reservoirs recover on centennial time scales, while SMP continue to cycle in air, soil, and surface ocean for millennia. Business as usual or maximum feasible reduction and discard scenarios show similar, 4-fold increases in atmospheric and aquatic ecosystem SMP exposure by 2050, because future plastics mobilization is controlled by releases from the large terrestrial discarded plastics reservoir. We conclude that in order to limit future dispersal of plastics we should, in addition to reducing plastics use and waste, anticipate remediation of the large terrestrial legacy plastics pool.

Methods

The GBM-Plastics-v1.0 model (global box model for plastics, version 1.0) code is included in SI 3 as Python scripts, and in SI 2 in a Microsoft© Excel© version. It is also available via https://github.com/AlkuinKoenig/GBM-Plastics. Definitions of plastics size categories are continuously debated; here we use operational definitions of macroplastics (P, >5mm), large microplastics (LMP, >0.3mm

and <5mm) and small microplastics (SMP, <0.3mm). The 0.3mm distinction is based on the frequently used plankton net mesh size of approximately 0.3 mm. The 0.3mm cut-off is also a reasonable starting point for the simulation of atmospheric cycling of SMP, with nearly all remote airborne SMP particles, films and 50% of fibers falling in the 1-300 µm range (5,24). All P, LMP, SMP reservoir sizes (i.e., inventory) and fluxes are expressed in teragrams (Tg = 10^{12} grams) and Tg y^{-1}. For some reservoirs, studies do not discern LMP or SMP, in which case we retain the generic 'MP' abbreviation.

LMP and SMP observations are typically expressed as MP counts per unit volume or per unit area. To estimate mass concentrations, we use, whenever reported, the full MP size distribution reported, a uniform density of 1 x 10^{-6} µg $µm^{-3}$ (41), and the MP volume approximation, V = L^3 x 0.1, where L are the reported length values of the size distribution.

We use global plastics production, 8300 Tg (teragrams or millions of metric tons), and waste generation (discarded, recycled or incinerated) from Geyer et al. (3). Produced plastics enter the 'in-use' pool, where they are mostly discarded within a single year due to the dominant use of single-use packaging. In 2015, 55% of non-fiber plastics are still discarded within a year, 25% incinerated and 20% recycled (3). We assume fiber plastics to undergo similar relative discarding and incineration fates, leading to a 'discarded P+MP' reservoir of 4900 Tg, an incinerated pool of 800 Tg (atmospheric CO_2) and an in-use pool of 2600 Tg in 2015 as described by Geyer et al.(3). Lau et al. (4) estimated the proportion of municipal solid waste that enters aquatic and terrestrial environments as primary LMP to be 14 ± 4 % in 2016, which we apply here to all discarded plastics (4). We therefore apply a primary f_{LMP} fraction of 0.14 and primary f_P fraction of 0.86 to estimate transfer from the in-use to discarded reservoir for the period 2050-2015. The following mass balance equations are defined for in-use and discarded pools:

$$\frac{d(P_{use})}{dt} = P_{prod} - f_{disc} \times P_{waste} - f_{inc} \times P_{waste} \quad \text{(Eq.1)}$$

Where P_{use} is the mass of total plastic (P + LMP) in use, P_{prod} the mass of total plastics produced (Tg y^{-1}), P_{waste} the mass of total plastic waste, and f_{disc}, and f_{inc} are the fractions of P_{use} that are discarded, incinerated and recycled.

$$\frac{d(P_{disc})}{dt} = f_{disc} \times P_{waste} \times f_P - k_{P-river} \times P_{disc} - k_{discP \to LMP} \times P_{disc} \quad \text{(Eq.2)}$$

Where P_{disc} is the mass of P discarded, f_P is the fraction of total plastic waste that are macroplastics, $k_{P\text{-}river}$ is the transfer coefficient for P to the ocean, via river runoff.

$$\frac{d(LMP_{disc})}{dt} = f_{disc} \times P_{waste} \times f_{LMP} + k_{discP \to LMP} \times P_{disc} - k_{LMP-river} \times LMP_{disc} - k_{discLMP \to sMP} \times LMP_{disc} \text{ (Eq.3)}$$

Where LMP_{disc} is the mass of LMP discarded, f_{LMP} is the fraction of total plastics waste that are primary microplastics (pellets, synthetic textiles, personal care products, etc), $k_{LMP\text{-}river}$ is the transfer coefficient for LMP to the ocean, via river runoff, and $k_{LMP \to SMP}$ is the transfer coefficient for LMP degradation to SMP within the terrestrial 'discarded' pool.

$$\frac{d(SMP_{disc})}{dt} = k_{discLMP \to SMP} \times SMP_{disc} - k_{SMP-river} \times SMP_{disc} - k_{disc-atm} \times SMP_{disc} \text{ (Eq.4)}$$

Where SMP_{disc} is the mass of SMP discarded, $k_{SMP\text{-}river}$ is the transfer coefficient for SMP to the ocean, via river runoff, and $k_{SMP\text{-}atm}$ is the transfer coefficient for SMP emission to the atmosphere from the terrestrial 'discarded' pool, including tire wear particles (TWP).

Transfer coefficients $k_{P\text{-}river}$, $k_{LMP\text{-}river}$, and $k_{SMP\text{-}river}$ are calculated from 2015 plastic fluxes and inventories, e.g. $k_{P\text{-}river}=P_{disc}/F_{P\text{-}river}$ where F stands for flux (SI 1, Table S1). The mid-point estimate for $F_{P\text{-}river}$ of 8.8 Tg y^{-1} ((11,42)) is used here, and subdivided into 50% P and 50% LMP (21). The 'discarded pool to atmosphere' transfer coefficient, $k_{disc\text{-}atm}$, which theoretically equals $SMP_{disc}/F_{SMP\_disc\text{-}atm}$ is unconstrained, because the SMP_{disc} pool size, in Tg, is unknown ($F_{SMP\_disc\text{-}atm}$ is 0.18 Tg y^{-1}, based on Brahney et al. (19), and was therefore fitted at 0.00037 y^{-1} as described in the text.

The global ocean. Two previous box models have examined the plastics budget of the marine environment (13,16). In addition, a number of Lagrangian oceanic or atmospheric transport models have provided insight in marine plastics dispersal and surface ocean plastics mass balance (15,19,43). Koelmans et al. (13) used a plastics mass budget for the surface ocean to fit a marine P to LMP fragmentation rate, and a LMP sedimentation rate, under the assumption of 100% buoyant P (no settling to deep waters). To accommodate the high river plastic inputs, rapid plastic fragmentation to LMP (>90% per year), and rapid LMP settling rates were fitted, and suggested a short plastics and LMP residence time for the surface ocean (<3 yrs). Subsequent modeling work has investigated P and LMP beaching, resuspension in coastal waters (15,16) , marine SMP emissions(19), and P sedimentation due to loss of buyuancy(16). Lebreton et al. (16), in their marine box model study(16), argued that observations of old plastics in the surface ocean disagree with rapid fragmentation and settling and fitted a plastics to LMP degradation rate of 3% per year, which we adopt here for the surface mixed layer ($k_{Poce \rightarrow LMP} = 0.03\ y^{-1}$).

Lebreton et al. (16) fitted important beaching of coastal plastics (97% per year). In the absence of a robust estimate for global beached macroplastics (44), Onink et al. (15) recently analyzed model beaching and resuspension scenarios finding at least 77% of net beaching for positively buoyant plastic debris over 5 years (15), which we adopt here in the base case as $k_{P,beaching} = 0.15\ y^{-1}$. Surface ocean P, LMP, and SMP equations are:

$$\frac{d(P_{surf-oce})}{dt} = k_{P-river} \times P_{disc} - k_{Psurf-oce-beach} \times P_{oce} - k_{Psurf-oce \rightarrow LMP} \times P_{surf-oce} - k_{Psurf-oce \rightarrow sed} \times P_{surf-oce} \times f_{shelf} \quad \text{(Eq.5)}$$

$$\frac{d(LMP_{surf-oce})}{dt} = k_{LMP-river} \times LMP_{disc} + k_{Psurf-oce \rightarrow LMP} \times P_{oce} - k_{LMPsurf-oce \rightarrow beach} \times LMP_{surf-oce} - k_{LMPsurf-oce \rightarrow shelfsed} \times LMP_{surf-oce} \times f_{shelf} - k_{LMP-sink} \times LMP_{surf-oce} \times f_{pelagic} - k_{LMPsurf-oce \rightarrow SMP} \times LMP_{surf-oce} \quad \text{(Eq.6)}$$

$$\frac{d(SMP_{surf-oce})}{dt} = k_{SMP-river} \times SMP_{disc} + k_{atm \rightarrow oce} \times SMP_{atm} + k_{terr \rightarrow oce} \times SMP_{terr} + k_{LMPsurf-oce \rightarrow SMP} \times LMP_{surf-oce} - k_{oce \rightarrow atm} \times SMP_{surf-oce} - k_{SMPsurf-oce \rightarrow sed} \times SMP_{surf-oce} \times f_{shelf} - k_{SMP-sink} \times SMP_{surf-oce} \times f_{pelagic} \quad \text{(Eq.7)}$$

$$\frac{d(P_{shelf-sed})}{dt} = k_{Psurf-oce \rightarrow sed} \times P_{surf-oce} \times f_{shelf} \quad \text{(Eq.8)}$$

$$\frac{d(LMP_{shelf-sed})}{dt} = k_{LMPsurf-oce \rightarrow sed} \times LMP_{surf-oce} \times f_{shelf} \quad \text{(Eq.9)}$$

$$\frac{d(SMP_{shelf-sed})}{dt} = k_{SMPsurf-oce \rightarrow sed} \times SMP_{surf-oce} \times f_{shelf} \quad \text{(Eq.10)}$$

Where $f_{shelf} = 0.08$, is the fraction of global continental shelf surface area, and $f_{pelagic}$ is the fraction of open ocean surface area. Subsurface ocean equations are:

$$\frac{d(LMP_{deep-oce})}{dt} = k_{LMP-sink} \times LMP_{surf-oce} \times f_{pelagic} - k_{LMP \rightarrow SMP} \times LMP_{deep-oce} - k_{LMPdeep \rightarrow deepsed} \times LMP_{deep-oce} \quad \text{(Eq.11)}$$

$$\frac{d(SMP_{deep-oce})}{dt} = k_{SMP-sink} \times SMP_{surf-oce} \times f_{pelagic} + k_{LMP \rightarrow SMP} \times LMP_{deep-oce} - k_{SMPdeep \rightarrow deepsed} \times SMP_{deep-oce} \quad \text{(Eq.12)}$$

$$\frac{d(P_{beach})}{dt} = k_{P-beach} \times P_{surf-oce} - k_{P \rightarrow LMP} \times P_{beach} \quad \text{(Eq.13)}$$

$$\frac{d(LMP_{beach})}{dt} = k_{LMP-beach} \times LMP_{surf-oce} + k_{P\rightarrow LMP} \times P_{beach} \quad \text{(Eq.14)}$$

$$\frac{d(LMP_{deep-sed})}{dt} = k_{LMP-sed} \times LMP_{surf-oce} \times f_{pelagic} \quad \text{(Eq.15)}$$

$$\frac{d(SMP_{deep-sed})}{dt} = k_{SMP-sed} \times SMP_{surf-oce} \times f_{pelagic} \quad \text{(Eq.16)}$$

Estimation of shelf sediment, deep sediment and beached P, and MP, based on reviews of literature data reporting MP counts per surface area and particle size statistics, is relatively straightforward. The beached MP pool is estimated at 0.5 Tg, based on the global surface of sandy beaches ($2.63 \cdot 10^5$ km^2; (28)), a median global beach sand MP abundance of 2450 MP km^{-2} (IQR, 613 – 2700), and median MP size of 2.0 mm (IQR, 1.1 – 3.8) (29). Reviews of deep ocean MP and shelf sediment MP pools report numbers of MP counts per mass unit, which leads to more intricate pool mass estimates: Barrett et al. (31) reported mean deep sediment MP concentrations of 0.72 MP g^{-1} for cored and grab sediment samples of 9cm depth. Deep sea sedimentation rates are typically on the order of 0.1-1 cm per 1000 years, suggesting that the majority of such composite sediment samples pre-date the plastics mass production period <1950. Yet, the measurement (0.72 MP g^{-1}) is expressed relative to the bulk of the composite sample mass, representing on average 9 cm of deep sea sediment (31). In this case we used the following data to estimate the global deep sea MP pool mass: depth in cm, dry sediment bulk density of 1.37 g cm^{-3}, a water to sediment mass ratio of 3.0, the mean MP size of 0.1 mm reported (31), a MP density of 1 x 10^{-6} µg µm^{-3}, and an open ocean seafloor surface area of 3.36 x 10^8 km^2. Similarly; the shelf sediment MP pool is estimated from subtidal sediment median MP concentrations of 100 MP kg^{-1} (IQR, 32-120), reviewed and reported by Shim et al. (29), a corresponding median MP size of 2.0 mm (IQR, 1.1 – 3.8), a dry sediment bulk density of 1.37 g cm^{-3}, a typical shelf sedimentation rate of 1 mm y^{-1}, 65 years of MP accumulation (1950 – 2015), a water to sediment mass ratio of 3.0, and a shelf seafloor surface area of 3.53 x 10^7 km^2. The final estimates for the deep ocean and shelf sediment MP pools are 1.5 Tg and 65 Tg (1σ, 21 to 78Tg) respectively. We acknowledge that plastic litter concentrates in given areas of the seafloor, and therefore, sediment sampling data could be biased depending on the sampling site. This is ultimately reflected in the large budget uncertainties.

The global atmosphere. Brahney et al. (19,24) estimated the global atmosphere to contain 0.0036 Tg of SMP. They also estimated global emissions from roads, 0.096 Tg y^{-1}, agricultural dust, 0.069 Tg y^{-1}, population dust, 0.018 Tg y^{-1}, and oceans, 8.6 Tg y^{-1}, which we adopt here. Atmospheric SMP deposition to remote terrestrial surfaces has been investigated by Allen et al. (5) in France, finding a median SMP deposition of 0.011 Mg km^{-2} y^{-1}, and by Brahney et al. (24). who observed a median of 0.0012 Mg km^{-2} y^{-1} in the western USA. Similar sampling and analysis techniques were used, and similar SMP particle and fiber size distributions found, suggesting that the 9x difference reflects the difference in population density of both areas, 100 inhabitants per km^2 in SW Europe vs. 16 per km^2 in the western USA. In (sub-)urban environments in Hamburg (Germany, 240 inhabitants per km^2) mean SMP deposition of 0.016 ± 0.006 Tg km^{-2} y^{-1} was observed (38). Precursor studies on atmospheric plastics observed mostly the LMP fiber fraction (0.3 to 5mm) with for example 0.014 Tg LMP km^{-2} y^{-1} in Dongguan (China) (23), but only 0.002 Tg km^{-2} y^{-1} in Paris (France) (22). For simplicity we do not include LMP emission to the atmosphere in the box model, since the short residence time of LMP likely leads to immediate deposition back to the broad terrestrial discarded LMP reservoir. We regress SMP deposition over land, from the three detailed recent studies mentioned above, as a function of population density (SI 1, Figure S1). We then extrapolate the observed relationship globally using population density and surface area data per country for the year 2015 (45), capping SMP deposition at 0.016 Tg km^{-2} y^{-1} based on the Hamburg observations. Doing so leads to a global SMP deposition estimate over land of 1.1 ± 0.5 Tg y^{-1}. SMP deposition over oceans is unconstrained by observations. We assume that global SMP emissions (8.6 Tg y^{-1}; (19)) equal deposition, and estimate SMP deposition over oceans to be 7.5 Tg y^{-1} (total deposition of 8.6– 1.1 Tg y^{-1} deposition over land).

The mass inventory, emission and deposition flux estimates for 2015 serve to approximate the mass transfer coefficients associated with emission, $k_{oce\rightarrow atm}$ and deposition, $k_{atm\rightarrow oce}$, $k_{atm\rightarrow terr}$, in the following mass balance equation:

$$\frac{d(SMP_{atm})}{dt} = k_{terr\rightarrow atm} \times SMP_{terr} + k_{disc\rightarrow atm} \times SMP_{disc} + k_{oce\rightarrow atm} \times SMP_{surf-oce} - k_{atm\rightarrow terr} \times SMP_{atm} - k_{atm\rightarrow oce} \times SMP_{atm} \quad \text{(Eq.17)}$$

We assume $k_{terr\rightarrow atm}$ to be equal to $k_{disc\rightarrow atm}$ which was derived from the modeled discarded SMP pool and the anthropogenic SMP emission flux of 0.18 Tg y^{-1} (sum of road, population and agricultural SMP emission) derived from the 3D global aerosol model for SMP dispersal by Brahney et al. (19).

Remote terrestrial pool. In the box model, agricultural and urban soils are included in the discarded plastics pool. We use a separate box for remote terrestrial surfaces, outside of the technosphere, that are solely supplied by atmospheric SMP. These include pristine soils, barren rock and land, ice sheets and remote inland waters. We estimate the approximate amount of SMP in the remote terrestrial pool by making use of the quasi-linear increase in global plastics production, discard and dispersal fluxes: global SMP deposition of 1.15 Tg y^{-1} in 2015 suggests a mean SMP deposition flux that is about half, 0.58 Tg y^{-1} since 1965, which multiplied by a land surface area of 1.49 10^8 km^2 amounts to 28 Tg of remote terrestrial SMP. SMP in this pool is mobilized by rainfall to river runoff to the surface ocean, with the same $k_{SMP\rightarrow river\text{-}oce}$ that we derived for SMP runoff from the discarded SMP pool. The remote terrestrial pool mass balance is:

$$\frac{d(SMP_{terr})}{dt} = k_{atm\rightarrow terr} \times SMP_{atm} - k_{terr\rightarrow atm} \times SMP_{terr} - k_{SMP\rightarrow river\rightarrow oce} \times SMP_{terr} \quad \text{(Eq. 18)}$$

BAU and SCS model scenarios. Both future, 2015 – 2050, model scenarios, business as usual (BAU), and systems change scenario (SCS, from Lau et al. (4)), use the same mass transfer coefficients, k, but different production, and waste management strategies summarized in the SI 2. BAU uses exponentially increasing production, and quasi-linearly increasing incineration and recycling, and decreasing discard from Geyer et al. (3). Lau et al. (4) developed a detailed model of plastics stocks and flows from municipal solid waste (MSW) and four sources of LMP. Their CSC scenario presents the most complete, yet feasible plastics management strategy over the period 2016 – 2040 for MSW, including a decrease in plastics production by 2040 to 220 Tg y^{-1}. We digitized their disposal (incineration + safe landfilling), recycling and discard model output (Tg y^{-1}), expressed these as fractions of MSW production, and extrapolated these to the year 2050 to compare to BAU. To do so, we anchored (by normalization) the SCS disposal fractions for the period 2015 – 2050 to the disposal fraction for 2050 – 2015 by Geyer et al.(3), in order to maintain a relatively smooth transition. We acknowledge that the SCS waste disposal estimates deviate to some extent from the original (4) estimates, but the overall trends are preserved: SCS disposal and recycling towards 2050 increase to 24 and 66 %, while discard declines to 10%. Extrapolation of current waste disposal trends under the BAU scenario leads to surprisingly similar numbers as SCS, though the real difference lies in the plastics production numbers that reach 991 Tg y^{-1} under BAU, and drop to 168 Tg y^{-1} in the SCS by 2050 (SI 2).

Budget and model uncertainty. The model assumes no temporal evolution of the mass transfer coefficients, k, implying that fragmentation, sedimentation, emission, deposition and release dynamics are considered time-invariant. While we argue that to first order these processes have remained similar through time, we acknowledge that reality is more complex. As more observational and mechanistic studies become available over the next decade, more appropriate parameterizations for plastics cycling can be tested, including the fragmentation of SMP to nanoplastics and ultimately dissolved and colloidal polymers with potential biological breakdown, i.e., as an energy source to biota.

Plastics data in the literature are predominantly reported as 'items per mass, volume, or surface area'. We converted these data to mass numbers by taking into account, where possible, the reported particle size distribution, or the reported median (or mean) particle size. In the case of fibers, reported length and diameter were used. Studies that did not report particle size properties were not included in the budget estimates. Particles were assumed to be flake shaped (46), with volume V defined as $V = L^3*0.1$, where L is the observed effective diameter, and have a mean density of 1 g cm^{-3}. In summary, for each particle size class, reported L was used to compute flake volumes, then multiplied by particle/fiber number, and multiplied by density to obtain particle/fiber mass. The obtained masses were summed to obtain total P, LMP or SMP mass in a sample.

Table 4 summarizes 1σ (one relative standard deviation, in %) expanded uncertainties of observed P, LMP and SMP pools (Tg) and fluxes (Tg y^{-1}), based on reported data, or conservatively approximated as

500%. The latter corresponds to a 2σ uncertainty of 1000%, which amounts to a factor 10. In other words, we consider that a large number of plastics pools and fluxes are at the moment only known to within a factor of 10. In the future, as more observations on plastics pools, fluxes and degradation become available, we will develop a formal Monte Carlo uncertainty analysis for the model.

Funding

We acknowledge financial support via the ANR-20-CE34-0014 ATMO-PLASTIC project, the Plasticopyr project within the Interreg V-A Spain-France-Andorra program, a CNRS 80prime PhD scholarship, and a MSCA ITN GMOS-Train PhD scholarship via grant agreement No 860497.

Acknowledgements

We thank the anonymous reviewers for their constructive comments, and K Mahowald for valuable discussion.

Author contributions

JES designed the study. JES, AK and JLT developed the model. All authors reviewed literature data, and contributed to model data interpretation and writing.

Availability of data and material

The authors declare that the data supporting the findings of this study are available within the paper and its supplementary information files.

Ethics approval and consent to participate

NA

Consent for publication

The authors provide consent for publication

Competing interests

The authors declare no competing financial or other interests.

References

1. Carpenter EJ, Smith KL. Plastics on the Sargasso sea surface. Science. 1972 Mar 17;175(4027):1240–1.

2. Hughes L, Rudolph J. Future world oil production: growth, plateau, or peak? Current Opinion in Environmental Sustainability. 2011 Sep 1;3(4):225–34.

3. Geyer R, Jambeck JR, Law KL. Production, use, and fate of all plastics ever made. Science Advances. 2017 Jul 19;3(7):e1700782.

4. Lau WWY, Shiran Y, Bailey RM, Cook E, Stuchtey MR, Koskella J, et al. Evaluating scenarios toward zero plastic pollution. Science. 2020 Sep 18;369(6510):1455–61.

5. Allen S, Allen D, Phoenix VR, Le Roux G, Durántez Jiménez P, Simonneau A, et al. Atmospheric transport and deposition of microplastics in a remote mountain catchment. Nat Geosci. 2019 May;12(5):339–44.

6. Peng X, Chen M, Chen S, Dasgupta S, Xu H, Ta K, et al. Microplastics contaminate the deepest part of the world's ocean. Geochemical Perspectives Letters. 2018 Nov 1;9:1–5.

7. Peeken I, Primpke S, Beyer B, Gütermann J, Katlein C, Krumpen T, et al. Arctic sea ice is an important temporal sink and means of transport for microplastic. Nat Commun. 2018 Apr 24;9(1):1505.

8. Woodall LC, Sanchez-Vidal A, Canals M, Paterson GLJ, Coppock R, Sleight V, et al. The deep sea is a major sink for microplastic debris. Royal Society Open Science. 2014 Dec 1;1(4):140317.

9. Koelmans AA, Redondo-Hasselerharm PE, Nor NHM, de Ruijter VN, Mintenig SM, Kooi M. Risk assessment of microplastic particles. Nat Rev Mater. 2022 Feb;7(2):138–52.

10. Eriksen M, Lebreton LCM, Carson HS, Thiel M, Moore CJ, Borerro JC, et al. Plastic Pollution in the World's Oceans: More than 5 Trillion Plastic Pieces Weighing over 250,000 Tons Afloat at Sea. PLOS ONE. 2014 Dec 10;9(12):e111913.

11. Jambeck JR, Geyer R, Wilcox C, Siegler TR, Perryman M, Andrady A, et al. Plastic waste inputs from land into the ocean. Science. 2015 Feb 13;347(6223):768–71.

12. Thompson RC, Olsen Y, Mitchell RP, Davis A, Rowland SJ, John AWG, et al. Lost at Sea: Where Is All the Plastic? Science. 2004 May 7;304(5672):838–838.

13. Koelmans AA, Kooi M, Law KL, Sebille E van. All is not lost: deriving a top-down mass budget of plastic at sea. Environ Res Lett. 2017 Nov;12(11):114028.

14. Kooi M, Nes EH van, Scheffer M, Koelmans AA. Ups and Downs in the Ocean: Effects of Biofouling on Vertical Transport of Microplastics. Environ Sci Technol. 2017 Jul 18;51(14):7963–71.

15. Onink V, Jongedijk CE, Hoffman MJ, Sebille E van, Laufkötter C. Global simulations of marine plastic transport show plastic trapping in coastal zones. Environ Res Lett. 2021 Jun;16(6):064053.

16. Lebreton L, Egger M, Slat B. A global mass budget for positively buoyant macroplastic debris in the ocean. Sci Rep. 2019 Sep 12;9(1):12922.

17. Long M, Moriceau B, Gallinari M, Lambert C, Huvet A, Raffray J, et al. Interactions between microplastics and phytoplankton aggregates: Impact on their respective fates. Marine Chemistry. 2015 Oct 20;175:39–46.

18. Lobelle D, Kooi M, Koelmans AA, Laufkötter C, Jongedijk CE, Kehl C, et al. Global Modeled Sinking Characteristics of Biofouled Microplastic. Journal of Geophysical Research: Oceans. 2021;126(4):e2020JC017098.

19. Brahney J, Mahowald N, Prank M, Cornwell G, Klimont Z, Matsui H, et al. Constraining the atmospheric limb of the plastic cycle. Proceedings of the National Academy of Sciences. 2021 Apr 20;118(16):e2020719118.

20. Allen S, Allen D, Moss K, Roux GL, Phoenix VR, Sonke JE. Examination of the ocean as a source for atmospheric microplastics. PLOS ONE. 2020 May 12;15(5):e0232746.

21. Weiss L, Ludwig W, Heussner S, Canals M, Ghiglione JF, Estournel C, et al. The missing ocean plastic sink: Gone with the rivers. Science. 2021 Jul 2;373(6550):107–11.

22. Dris R, Gasperi J, Saad M, Mirande C, Tassin B. Synthetic fibers in atmospheric fallout: A source of microplastics in the environment? Marine Pollution Bulletin. 2016 Mar 15;104(1):290–3.

23. Cai L, Wang J, Peng J, Tan Z, Zhan Z, Tan X, et al. Characteristic of microplastics in the atmospheric fallout from Dongguan city, China: preliminary research and first evidence. Environ Sci Pollut Res. 2017 Nov 1;24(32):24928–35.

24. Brahney J, Hallerud M, Heim E, Hahnenberger M, Sukumaran S. Plastic rain in protected areas of the United States. Science. 2020 Jun 12;368(6496):1257–60.

25. Allen S, Allen D, Baladima F, Phoenix VR, Thomas JL, Le Roux G, et al. Evidence of free tropospheric and long-range transport of microplastic at Pic du Midi Observatory. Nat Commun. 2021 Dec 21;12(1):7242.

26. Evangeliou N, Grythe H, Klimont Z, Heyes C, Eckhardt S, Lopez-Aparicio S, et al. Atmospheric transport is a major pathway of microplastics to remote regions. Nat Commun. 2020 Jul 14;11(1):3381.

27. Poulain M, Mercier MJ, Brach L, Martignac M, Routaboul C, Perez E, et al. Small Microplastics As a Main Contributor to Plastic Mass Balance in the North Atlantic Subtropical Gyre. Environ Sci Technol. 2019 Feb 5;53(3):1157–64.

28. Almar R, Ranasinghe R, Bergsma EWJ, Diaz H, Melet A, Papa F, et al. A global analysis of extreme coastal water levels with implications for potential coastal overtopping. Nature Communications. 2021 Jun 18;12(1):3775.

29. Shim WJ, Hong SH, Eo S. Chapter 1 - Marine Microplastics: Abundance, Distribution, and Composition. In: Zeng EY, editor. Microplastic Contamination in Aquatic Environments [Internet]. Elsevier; 2018 [cited 2022 Apr 11]. p. 1–26. Available from: https://www.sciencedirect.com/science/article/pii/B9780128137475000011

30. Haarr ML, Falk-Andersson J, Fabres J. Global marine litter research 2015–2020: Geographical and methodological trends. Science of The Total Environment. 2022;820:153162.

31. Barrett J, Chase Z, Zhang J, Holl MMB, Willis K, Williams A, et al. Microplastic Pollution in Deep-Sea Sediments From the Great Australian Bight. Frontiers in Marine Science [Internet]. 2020 [cited 2022 Apr 12];7. Available from: https://www.frontiersin.org/article/10.3389/fmars.2020.576170

32. Artham T, Sudhakar M, Venkatesan R, Madhavan Nair C, Murty KVGK, Doble M. Biofouling and stability of synthetic polymers in sea water. International Biodeterioration & Biodegradation. 2009 Oct 1;63(7):884–90.

33. Chamas A, Moon H, Zheng J, Qiu Y, Tabassum T, Jang JH, et al. Degradation Rates of Plastics in the Environment. ACS Sustainable Chem Eng. 2020 Mar 9;8(9):3494–511.

34. Eo S, Hong SH, Song YK, Han GM, Seo S, Shim WJ. Prevalence of small high-density microplastics in the continental shelf and deep sea waters of East Asia. Water Research. 2021 Jul 15;200:117238.

35. Courtene-Jones W, Quinn B, Gary SF, Mogg AOM, Narayanaswamy BE. Microplastic pollution identified in deep-sea water and ingested by benthic invertebrates in the Rockall Trough, North Atlantic Ocean. Environmental Pollution. 2017 Dec 1;231:271–80.

36. Pabortsava K, Lampitt RS. High concentrations of plastic hidden beneath the surface of the Atlantic Ocean. Nat Commun. 2020 Aug 18;11(1):4073.

37. Zhao S, Zettler ER, Bos RP, Lin P, Amaral-Zettler LA, Mincer TJ. Large quantities of small microplastics permeate the surface ocean to abyssal depths in the South Atlantic Gyre. Glob Chang Biol. 2022 May;28(9):2991–3006.

38. Klein M, Fischer EK. Microplastic abundance in atmospheric deposition within the Metropolitan area of Hamburg, Germany. Science of The Total Environment. 2019 Oct 1;685:96–103.

39. The World Bank. Population density data [Internet]. 2021 [cited 2022 Apr 11]. Available from: https://data.worldbank.org/indicator/EN.POP.DNST

40. Brahney Janice, Mahowald Natalie, Prank Marje, Cornwell Gavin, Klimont Zbigniew, Matsui Hitoshi, et al. Constraining the atmospheric limb of the plastic cycle. Proceedings of the National Academy of Sciences. 2021 Apr 20;118(16):e2020719118.

41. Kooi M, Koelmans AA. Simplifying Microplastic via Continuous Probability Distributions for Size, Shape, and Density. Environ Sci Technol Lett. 2019 Sep 10;6(9):551–7.

42. Lebreton LCM, van der Zwet J, Damsteeg JW, Slat B, Andrady A, Reisser J. River plastic emissions to the world's oceans. Nat Commun. 2017 Jun 7;8(1):15611.

43. Sebille E van, Wilcox C, Lebreton L, Maximenko N, Hardesty BD, Franeker JA van, et al. A global inventory of small floating plastic debris. Environ Res Lett. 2015 Dec;10(12):124006.

44. Browne MA, Chapman MG, Thompson RC, Amaral Zettler LA, Jambeck J, Mallos NJ. Spatial and Temporal Patterns of Stranded Intertidal Marine Debris: Is There a Picture of Global Change? Environ Sci Technol. 2015 Jun 16;49(12):7082–94.

45. World Bank. Population density [Internet]. 2021. Available from: https://www.worldbank.org/en/home

46. Cózar A, Echevarría F, González-Gordillo JI, Irigoien X, Úbeda B, Hernández-León S, et al. Plastic debris in the open ocean. Proceedings of the National Academy of Sciences. 2014 Jul 15;111(28):10239–44.

47. Ross PS, Chastain S, Vassilenko E, Etemadifar A, Zimmermann S, Quesnel SA, et al. Pervasive distribution of polyester fibres in the Arctic Ocean is driven by Atlantic inputs. Nature Communications. 2021 Jan 12;12(1):106.

48. Kanhai LDK, Gårdfeldt K, Lyashevska O, Hassellöv M, Thompson RC, O'Connor I. Microplastics in sub-surface waters of the Arctic Central Basin. Marine Pollution Bulletin. 2018 May 1;130:8–18.

49. Tekman MB, Wekerle C, Lorenz C, Primpke S, Hasemann C, Gerdts G, et al. Tying up Loose Ends of Microplastic Pollution in the Arctic: Distribution from the Sea Surface through the Water Column to Deep-Sea Sediments at the HAUSGARTEN Observatory. ENVIRONMENTAL SCIENCE & TECHNOLOGY. 2020 Apr 7;54(7):4079–90.

627 **Table 1. Subsurface ocean microplastics (MS) observations.** MS include fragments and fibers in the 0.3 –
628 5 mm (LMP) and <0.3 mm (SMP) range. Reported data in # m^{-3} were converted to mass concentrations, taking
629 into account the full particle/fiber size distribution (see Methods).

Ocean basin	**Location**	**depth**	**LMP+SMP**	**Reference**
		m	µg m^{-3}	
N-Pacific	Korean East Sea	206	125	(34)
N-Pacific	Korean East Sea	2100	177	(34)
N-Pacific	Mariana Trench	2673	90	(6)
Mean			**131**	
1σ			44	
N- and S-Atlantic	-53º S to 47º N	160	134	(36)
N-Atlantic	Rockall Trough	2200	97	(35)
S-Atlantic	Gyre		43	(37)
Mean			**91**	
1σ			46	
Arctic Ocean	Central basin	5 to 1000	6	(47)
Arctic Ocean	Central basin	1769	66	(48)
Arctic Ocean	Fram Strait	300 to 5570	0.2	(49)
Mean			**24**	
1 σ			36	

630

Table 2. Global subsurface ocean microplastics budget. Atlantic, N-Pacific and Arctic Ocean data from Table 1. Microplastics (MP) include fragments and fibers in the 0.3 – 5 mm (LMP) and <0.3 mm (SMP) range. Data for the S-Pacific and Southern Ocean are extrapolated based on surface Ocean data from Shim et al.(29) with uncertainties set to 10x. No data exists for the Indian Ocean, where concentrations were assumed equal to the S-Atlantic observations by Eo et al.(34)(Table 1). Subsurface oceanic budgets in Tg include do not include the mixed layer (upper 0.1 km).

Ocean basin	**Area**	**Volume**	**MP**	**MP**	**1σ**
	km^2	km^3	$\mu g\ m^{-3}$	Tg	Tg
Arctic Ocean	15558000	18750000	24	0.4	0.6
North Atlantic	41490000	146000000	91	13.0	3.0
South Atlantic	40270000	160000000	91	14.3	3.3
Indian Ocean	70560000	264000000	43	11.0	11.0
North Pacific	77010000	331000000	131	42.2	14.1
South Pacific	84750000	329000000	4	1.2	12.0
Southern Ocean	21960000	71800000	4	0.3	3.0
Total				**82**	**47**

Table 3. Atmospheric small microplastics (SMP) budget. Mean ± 1σ SMP concentrations in the BL (boundary layer) (144 ± 124 ng m^{-3} for outdoors locations) and FT (free troposphere) (0.3 ± 0.2 ng m^{-3}) are from Allen et al. (25), assuming a mean SMP size of 70 μm for SMP in the BL, based on Brahney et al. (19).

	Mean global BL height	**Mean global FT height**	**Area**	**BL SMP**	**FT SMP**
	km	km	km^2	Tg	Tg
ocean	0.25	13	$3.62\ 10^8$	0.013	0.0014
land	0.75	13	$1.48\ 10^8$	0.016	0.0005
Total				0.031	

644 **Table 4. Comparison of observed and modeled plastics mass (M, in Tg) and fluxes (F, in Tg y^{-1}) for the**
645 **year 2015.** Plastics are divided in macroplastics, P (>5 mm), large microplastics, MP (0.3 – 5mm), and small
646 microplastics, SMP (<0.3 mm). Uncertainties (1σ) on observations are based on the literature, except when
647 not reported, in which case we assigned an uncertainty, denoted by '*'. Uncertainties (1σ) on model estimated
648 pools and fluxes are conservatively estimated to be 500% (denoted by '**'), corresponding to a 2σ uncertainty
649 of a factor of 10 (see Methods). The first column with M and F abbreviations correspond to parameter
650 nomenclature used in mass balance equations 1-18.

Reservoir mass (M) or flux (F)	Abbreviation	Observed	Uncertainty	Box model
			1σ	
M P produced	P_{prod}	8300	10%*	8300
M P in-use	P_{use}	2600	10%*	3320
M P discarded	P_{disc}	4214	22%	2382
M LMP discarded	LMP_{disc}	686	22%	1222
M SMP discarded	SMP_{disc}			540**
M P Surface Ocean	$P_{surf\text{-}oce}$	0.23	75%*	0.021
M LMP Surface Ocean	$LMP_{surf\text{-}oce}$	0.031	75%*	0.038
M SMP Surface Ocean	$SMP_{surf\text{-}oce}$	0.0028	196%	0.009
M LMP Deep Ocean	$LMP_{deep\text{-}oce}$	82	57%	77
M SMP Deep Ocean	$SMP_{deep\text{-}oce}$			33
M SMP atmosphere	SMP_{atm}	0.03	500%	0.011
M SMP remote terrestrial	SMP_{terr}	28	37%	41
M P beach	P_{beach}	1.3	500%*	1.1
M LMP beach	LMP_{beach}	0.53	100%	2.9
M P shelf sediment	$P_{shelf\text{-}sed}$	51	500%*	43
M LMP shelf sediment	$LMP_{shelf\text{-}sed}$	65	100%	9.5
M SMP shelf sediment	$SMP_{shelf\text{-}sed}$			0.3**
M LMP deep ocean sediment	$LMP_{deep\text{-}sed}$	1.0	500%*	1.2
M SMP deep ocean sediment	$SMP_{deep\text{-}sed}$			0.1
M P Incinerated	P_{incin}	800	20%*	626
M P Recycled	P_{recyc}	750	20%*	554
F P_{use} to LMP_{disc}		42	22%	41
F P_{use} to P_{disc}		118	22%	130
F P_{use} to P_{incin}		74	20%*	63
F P_{use} to P_{recyc}		56	20%*	57
F P_{disc} to LMP_{disc}				71**
F LMP_{disc} to SMP_{disc}				36**
F P river				2.4**
F LMP river				7.5**
F SMP river (from SMP_{disc})				3.3**
F SMP river (from P_{terr})				0.3**
F river total		0.006-13		13
F Surface Ocean P to LMP				0.001**
F Surface Ocean LMP to SMP				0.001**
F Deep Ocean LMP to SMP				2.3**
F SMP Ocean to atmosphere		8.6	500%*	27
F SMP Atmosphere to ocean		7.6	500%*	23
F P beaching				0.1**
F LMP beaching				0.2**
F beach P to LMP				0.03**
F LMP surface to deep ocean				6.8**
F SMP surface to deep ocean				0.3**
F P surface to shelf sediments				2.3**
F LMP surface to shelf sediments				0.6**
F SMP surface to shelf sediments				0.02**
F LMP deep ocean to sediments				0.1**
F SMP deep ocean to sediments				0.01**
F SMP terrestrial to atmosphere				0.01**

F SMP atm to terrestrial pool		1.1	37%	3.5
F SMP Discard to atmosphere		0.183	500%*	0.2

Figures

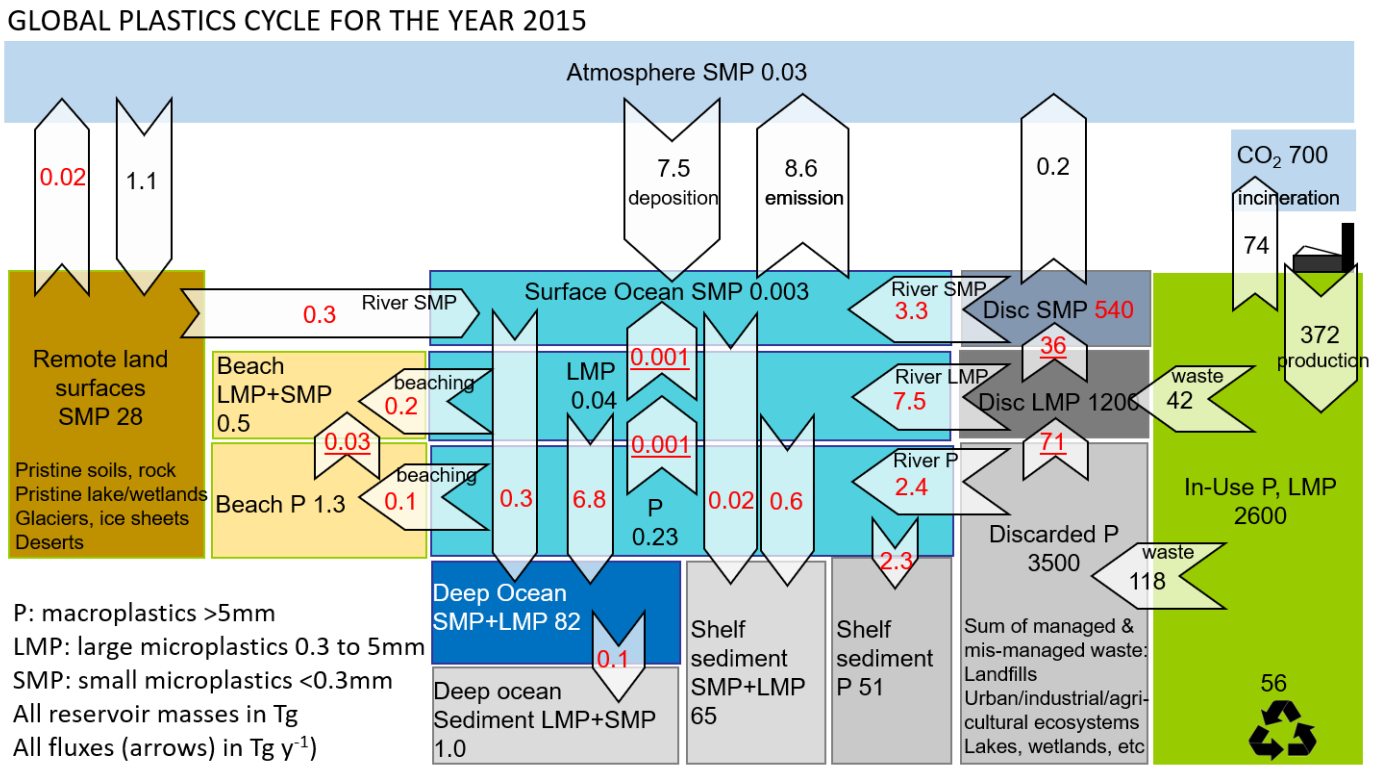

Figure 1. Global plastics budget and cycle for the year 2015 based on best-available observations and model estimates. Reservoir sizes are shown in teragrams (Tg), and fluxes in Tg y^{-1} (arrows). Three plastics size classes are considered: macroplastics > 5mm (P), microplastics from 0.3 to 5mm (LMP), and small microplastics <0.3mm (SMP) that can become airborne. The discarded (Disc) plastic pools represent the terrestrial technosphere, where managed and mismanaged waste has accumulated in urban-industrial areas, landfills, agricultural soils impacted by mulching or waste disposal, wetlands, lakes and other ecosystems. The remote terrestrial reservoir lies outside the technosphere and is only impacted by airborne SMP deposition, re-emission and runoff. Numbers in black are based on observations, and numbers in red on the box model simulation. Underlined red fluxes indicate P and LMP degradation at a rate of 3% per year. Uncertainties are provided in Table 4. Note that such the 2015 global budget is not at steady-state and fluxes and pool sizes continue to gradually increase today and in the future.

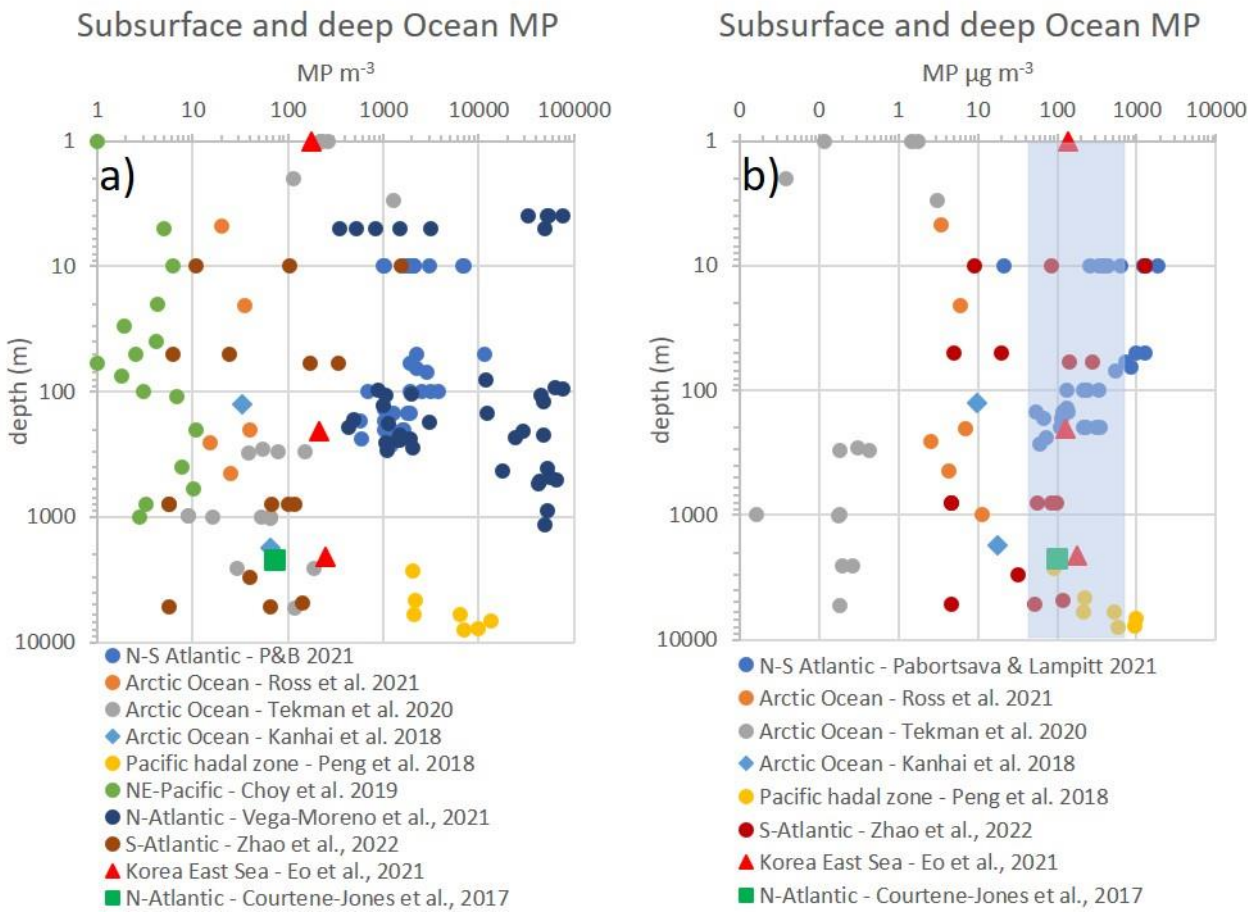

Figure 2. Subsurface Ocean microplastics (MP=LMP+SMP) observations. (**A**) MP number concentrations per m^3 of sea water. (**B**) MP mass concentrations for datasets where particle/fiber size distribution was reported (see Methods). The shaded vertical bar indicates the range of mean ± 1σ mass concentrations estimated for the Pacific and Atlantic Oceans (45 to 175 µg m^{-3}, Table 1).

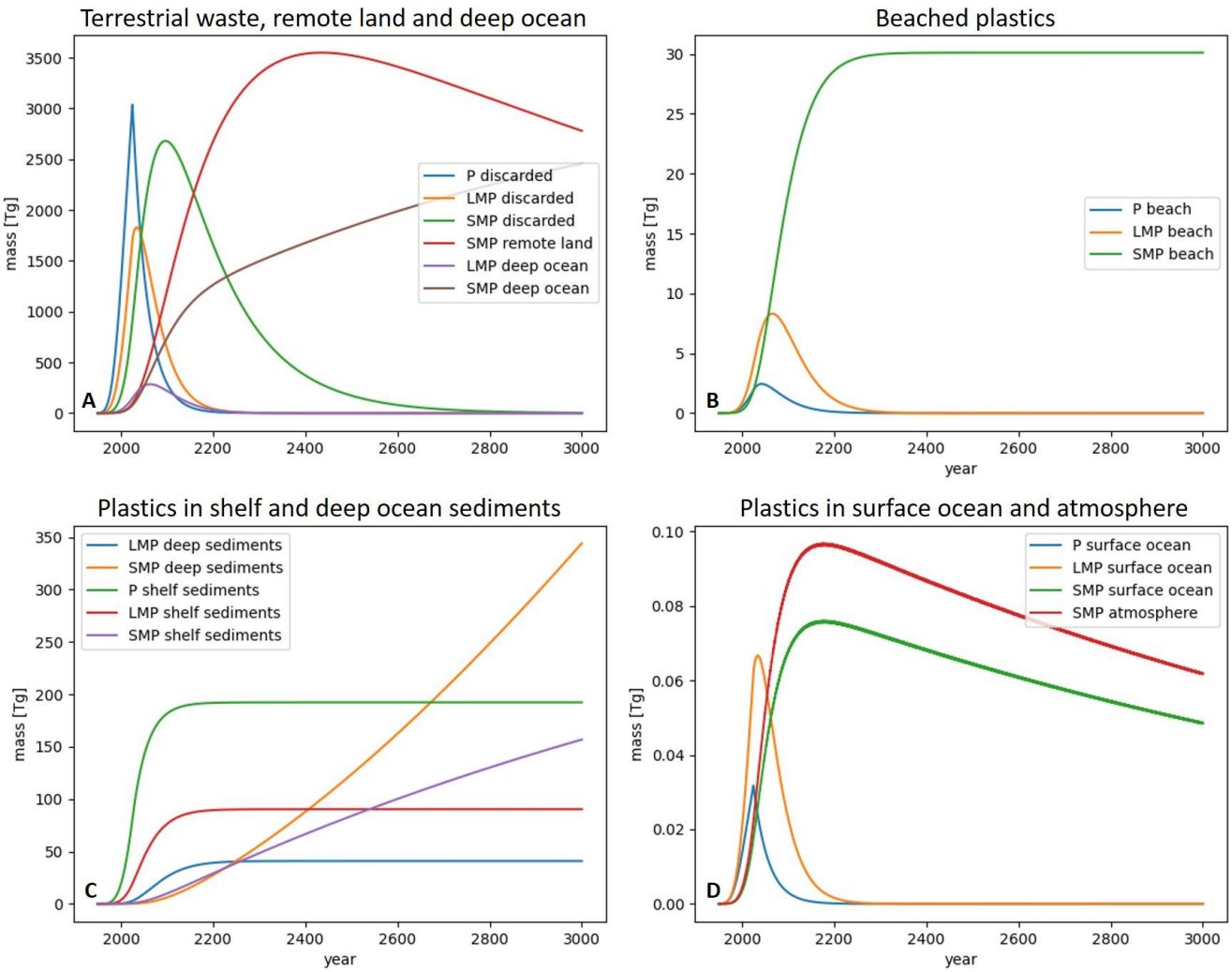

Figure 3. Plastics dispersal through Earth surface reservoirs from 1950 to the year 3000, following a halt on production and discard in 2025. This unrealistic model scenario illustrates over what timescales discarded microplastic (P, >5mm), large microplastic (LMP) and small microplastic (SMP, <0.3mm) potentially disperse via rivers and air into oceans, remote terrestrial surfaces, beach and marine sediments. (**A**) P and LMP disappear in all transitory reservoirs within 100 and 200 years due to fragmentation at an annual rate of 3%. The prolonged dispersal of SMP in all reservoirs is driven by cyclical marine emissions to air, deposition to terrestrial surfaces, runoff to surface oceans, and re-emission to air. Only a small fraction of SMP sinks to shelf sediments and to the deep ocean, followed by slow sedimentation to deep ocean sediments. SMP mass, and concentrations, in the surface ocean and atmosphere, where human SMP exposure is relevant, only return to 2025 levels towards the year 5000 (Figure 4).

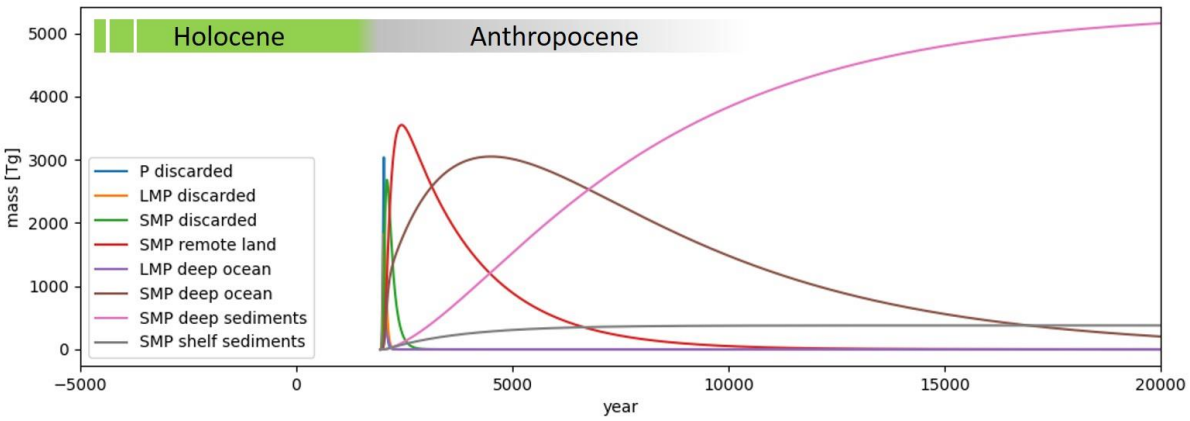

683

684 **Figure 4. Plastics dispersal through Earth surface reservoirs from 1950 to the year 20,000 CE, following**
685 **a halt on production and discard in 2025.** This is the same model scenario that is shown in Figure 3, and
686 illustrates over what timescales discarded microplastic (P, >5mm), large microplastic (LMP) and small
687 microplastic (SMP, <0.3mm) potentially disperse via rivers and air into oceans, remote terrestrial surfaces,
688 and marine sediments. P and LMP disappear in all transitory reservoirs within 100 and 200 years due to
689 fragmentation at an annual rate of 3%. The prolonged dispersal of SMP in all reservoirs is driven by cyclical
690 marine emissions to air, deposition to terrestrial surfaces, runoff to surface oceans, and re-emission to air.
691 Only a small fraction of SMP sinks to shelf sediments and to the deep ocean, followed by slow sedimentation
692 to deep ocean sediments.

693

694

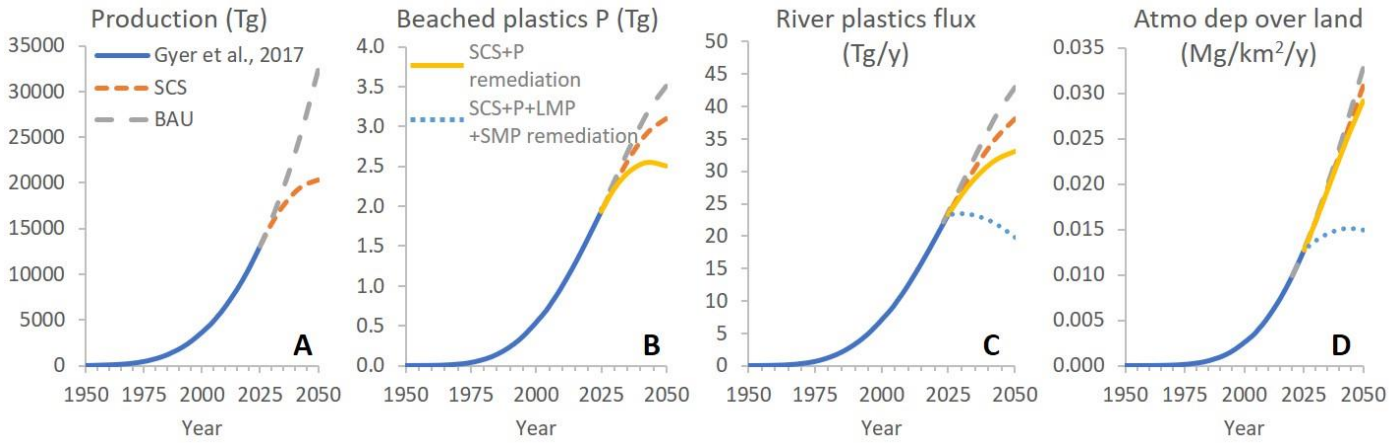

Figure 5. Box model results for plastics cycling from 1950 to 2050. From 1950 to 2015 the model estimates the dispersal of P, LMP and SMP in different Earth surface reservoirs, based on known plastics production and waste generation. From 2015 to 2050 the model illustrates plastics production (**A**), amount of beached macroplastics, P (**B**), the total, P+LMP+SMP, annual river plastics flux (**C**), and atmospheric deposition (atmo dep) to remote land surfaces (**D**), for two different scenarios with different plastics production and waste disposal trajectories: business as usual (BAU, grey dashed line) (3), and systems change scenario (SCS, orange short dashed line) (4), the latter representing feasible plastics policy implementation. Despite the large difference in plastics production towards 2050, 991 vs 168 Tg y^{-1} in BAU and SCS, environmental stocks and fluxes recover only slowly due to the large mobilization of mismanaged plastics from the terrestrial discarded plastics pool that continue to cycle between land, ocean and atmosphere. Two remediation scenarios are simulated for the 2025 to 2050 period: Discarded P remediation at a rate of 3% per year (yellow solid line), and combined discarded P, LMP and SMP remediation at a rate of 3% per year. See Methods and SI 2 for details on BAU and SCS.